THE JOURNAL OF BIOLOGICAL CHEMISTRY
Vol. 275, No. 52, Issue of December 29, pp. 41028–41034, 2000

Printed in U.S.A.

Dynamic Shuttling of Nuclear Factor κB between the Nucleus and Cytoplasm as a Consequence of Inhibitor Dissociation*

Received for publication, July 13, 2000, and in revised form, September 27, 2000
Published, JBC Papers in Press, October 6, 2000, DOI 10.1074/jbc.M006179200

Franco Carlotti‡, Steven K. Dower‡, and Eva E. Qwarnstrom‡§¶

From the ‡Functional Genomics Group, Division of Molecular and Genetic Medicine, Royal Hallamshire Hospital, University of Sheffield, Glossop Road, Sheffield S10 2JF, United Kingdom and the §Department of Pathology, University of Washington, Seattle, Washington 98195-7470

Activation of the nuclear factor κB (NFκB) transcription factor is intimately associated with its translocation from the cytoplasm to the nucleus. Using the nuclear export inhibitor leptomycin B, we demonstrate shuttling of the RELA subunit of NFκB and the inhibitory subunit IκBα between these two compartments in unstimulated cells. Determination of the kinetics of nuclear entry shows marked differences for the two components; the entry of IκBα occurs more rapidly than RELA. The shuttling is suggested to be a consequence of the cytoplasmic dissociation of the NFκB·IκB complex rather than its direct nuclear import or degradation and resynthesis of IκBα. Using previously published kinetic data, this proposition is born out by the deduction that 17% of NFκB is not complexed to IκBα in a resting cell. A numerical model is presented to validate the proposed regulation of NFκB subcellular localization consequent in part on the nuclear export function and in part on the cytoplasmic retention function of IκBα. We suggest that the non-saturated interaction of NFκB with the inhibitor may enhance the specificity of action of IκB proteins on different NFκB dimers and allow additional modes of regulation of IκB function.

NFκB[1] is a central mediator of immune and inflammatory responses. It consists of homo- or heterodimers of a family of at least five related proteins characterized by the rel homology domain (1, 2). The known members of this family are c-REL, RELA, RELB, p50, and p52. Homodimers of p50 and p52 are generally considered to be inhibitory, because they lack activation domains, but they may be converted to activators by association with the Bcl3 protein (3, 4). NFκB is regulated by a family of at least seven inhibitory proteins, IκB, characterized by multiple ankyrin-type repeats (5). The expression of both NFκB and IκB proteins is cell type- and developmental stage-specific (2). In non-lymphomyeloid cells, the most prevalent NFκB species are RELA-p50 heterodimers and p50 homodimers.

The current model for NFκB function postulates that the transcription factor is anchored in the cytoplasm by association with the inhibitor in unstimulated cells (6). Whereas both NFκB and IκB have nuclear localization signals, resulting in import of the free factors to the nucleus, these are mutually masked within the complex to abolish their nuclear import functions (7). A diverse range of stimuli, including inflammatory cytokines, bacterial lipopolysaccharide, and phorbol esters (8–10), result in the serine phosphorylation of IκB and its subsequent degradation (11, 12). Translocation of the free transcription factor to the nucleus and activation of genes bearing cognate binding sites ensues. Tyrosine phosphorylation of IκBα, without subsequent degradation, has also been reported to release active NFκB into the nucleus (13). In addition to nuclear translocation, phosphorylation of NFκB may be important for its full activation (14–17). This phosphorylation may be induced by parallel pathways initiated by the same stimulus as that causing IκB degradation.

We have previously developed quantitative green fluorescent protein-based assays to determine the activation of NFκB in single, living cells (18). These experiments demonstrated activation by IL-1 to be dependent on the level of NFκB expression. In particular, as the expression level of NFκB increased, its rate of nuclear translocation saturated at approximately 60 molecules per s. The location of the rate-limiting step was proposed to lie within the signal transduction cascade. In this paper, we examine how the kinetics of activation are modified when nuclear export of NFκB/IκB is blocked using the specific inhibitor of CRM1-dependent nuclear export leptomycin B (LMB) (19, 20). These data demonstrate a greater importance for nuclear export function of IκBα in maintaining a low basal activity of nuclear NFκB than has previously been supposed. We have developed a numerical model to test this mechanism of NFκB regulation against our observations.

EXPERIMENTAL PROCEDURES

Plasmids *pEGFP-RELA* (18), *pECFP-RELA*[2], *pIκBαEGFP*[2], and *pIκBαEYFP*[2] elsewhere described. *pCMV-RELA* was constructed by digesting the plasmid *pEGFP-RELA* with *Hin*dIII plus *Nhe*I, infilling with Klenow polymerase, and then religating. Interleukin 1β was a gift of the Immunex Corporation, and LMB was a gift of Dr. Minoru Yoshida. Cycloheximide was obtained from Sigma, and MG132 was from Calbiochem.

Cell Culture—Monkey arterial smooth muscle cells were maintained in Dulbecco's modified Eagle's medium (Life Technologies, Inc.) containing 10% fetal calf serum (Life Technologies, Inc.) and used between transfers 9 and 13. For microscopic assays, 20,000 cells were plated in four-chamber coverslips (NUNC) 2 days prior to transfection with 2 μg of plasmid DNA by calcium phosphate co-precipitation as described previously (18). For studies involving IκBα·EGFP, the plasmid was co-transfected with *pCMV-RELA* to achieve cytoplasmic localization.[2] Co-transfection of IκBα with EGFP·RELA was not necessary because EGFP·RELA induces expression of the endogenous IκBα gene (21, 22). For the ECFP·RELA/IκBα·EYFP cotransfection studies, the plasmid

* This work was funded by the British Heart Foundation. The confocal microscopy facility was co-funded by the Wellcome Trust and the Medical Research Council. The costs of publication of this article were defrayed in part by the payment of page charges. This article must therefore be hereby marked "*advertisement*" in accordance with 18 U.S.C. Section 1734 solely to indicate this fact.

¶ To whom correspondence should be addressed. Tel.: 44-114-271-3181; Fax: 44-114-271-3846; E-mail: E.Qwarnstrom@Sheffield.ac.uk.

[1] The abbreviations used are: NFκB, nuclear factor κB; IκB, inhibitor of κB; IL, interleukin; LMB, leptomycin B; EGFP, enhanced green fluorescent protein; ECFP, enhanced cyan fluorescent protein; EYFP, enhanced yellow fluorescent protein.

[2] L. Yang, F. Carlotti, and E. E. Qwarnstrom, manuscript in preparation.

ratio was varied from 1:1 to 1:4 to allow the analysis of cells with high concentrations of free IκBα·EYFP. Analysis of IL-1/LMB stimulation of IL-6 production was performed on cells plated in 24-well tissue culture dishes (75% confluent, plated 48 h prior to stimulation). The concentration of IL-6 in the supernatant was determined at the end point by enzyme-linked immunosorbent assay (Quantikine, R & D Systems Inc.).

Microscopy—EGFP·RELA and IκBα·EGFP were visualized using a Molecular Dynamics confocal laser scanning microscope with a 37 °C stage incubator. The images were analyzed as described previously (18) to yield parameter values as described below. The microscopy was performed with standardized laser power (10 mW) and photomultiplier tube (667 V) settings but variable attenuation of the incident laser beam to allow on-scale recordings of both bright and faintly fluorescent cells. Fluorescence units are defined as the pixel density of the image divided by the percentage attenuation of the incident laser illumination and as such are directly proportional to EGFP fusion protein concentration. The nuclear import rate is defined as the absolute rate of increase in nuclear fluorescence during the approximately linear phase (*i.e.* exclusive of the initial lag and later plateau stages). The relative nuclear import rate is defined as the nuclear import rate divided by the initial cytoplasmic fluorescence; the advantage of this measure is that it is independent of the expression level when the EGFP fusion is expressed at levels that do no perturb the endogenous system. The final measurement that we use is relative fluorescent units when presenting average time courses. These are calculated by dividing each measurement for a single cell by the initial cytoplasmic fluorescence of that cell and then averaging the values for the group of cells. This method has the advantages that the cells are equally weighted in the final curve and that meaningful standard deviations can be calculated. ECFP·RELA and IκBα·EYFP were visualized using a C4743–95 12-bit Hamamatsu digital camera driven by OpenLab software (Improvision) with the specific filter sets XF114 and XF104 (Omega Optical). Note that the fluorescent units for these proteins are not identical with those obtained for EGFP, because their excitation/detection characteristics differ.

Modelling—Numerical modelling was performed using an iterative model developed in the Microsoft EXCEL VBA programming language (available on request). For simplicity, the model treats NFκB and IκB as a single species partitioning between nuclear and cytoplasmic compartments. All parameter values are entered at run time using a simple user interface. Initial parameter values were estimated according to our data and previous reports as follows. To assign NFκB concentrations, we used our previous estimate for the concentration of RELA at 60,000 molecules per cell. Because the levels of IκB are regulated by free NFκB, IκB is assumed to be present in 10% excess relative to NFκB. We use the dissociation constant (k_{off}/k_{on}) for the interaction of the p50/RELA dimer with IκBα (3 nM (23)) because this is the highest affinity complex and is likely to be predominant in smooth muscle cells. The ratio of import/export rates (k_{imp}/k_{exp}) for IκBα was taken to be 2, because on gross overexpression of IκBα·EGFP, when it is likely to be present largely free of NFκB, it partitions with a 2:1 nuclear:cytoplasmic ratio. Because grossly overexpressed EGFP·RELA is substantially nuclear, the ratio of k_{imp}/k_{exp} for NFκB was taken to be 50. For assignment of absolute import and export rates, we have used k_{on} and k_{off} values for the NFκB·IκB complex of 18,400,000 M^{-1} min^{-1} and 0.055 min^{-1}, respectively (23), which constrains the nuclear import rates for consistency with the observed resting partitioning of NFκB/IκB and their rates of nuclear import following LMB treatment (these rates are determined by running the model). For the purpose of testing the model, we have assumed that the direct import of NFκB·IκB into the nucleus is not significant.

RESULTS

We have previously reported that IL-1-stimulated nuclear translocation of EGFP·RELA is impaired at high expression levels (18). This impairment might be caused by overexpression or rapid resynthesis of IκBα in the transfected cells, saturation of the nuclear import machinery, or kinetic limitations of the signal transduction pathway. To explore these possibilities, we have investigated the consequences for IL-1-induced import of blocking the nuclear export pathway using the specific inhibitor LMB. Treatment of cells with LMB alone resulted in the nuclear accumulation of EGFP·RELA (Fig. 1*A*), which indicates that, even in resting cells, EGFP·RELA cycles between the cytoplasm and nucleus. The rate of LMB-induced nuclear translocation of EGFP·RELA is lower than that induced by IL-1 in cells expressing physiological levels of the fusion protein. Furthermore, whereas the LMB-induced translocation is almost linear during the first 60 min of treatment (Fig. 1*B*) and displays minimal lag time, the IL-1-induced response has a distinct lag phase and attains a plateau. The time course of nuclear translocation in cells treated with both IL-1 and LMB also shows a plateau but at a level (6-fold above the initial cytoplasmic concentration) that is more than additive than for LMB and IL-1 alone (1.3× at 60 min and 2.5×, respectively). This level of nuclear translocation depletes approximately 70% of cytoplasmic EGFP·RELA.

To clarify the difference in response to IL-1 and LMB, we determined how the rate of nuclear translocation in individual cells varies according to the expression level of EGFP·RELA (Fig. 1*C*). Whereas the response to IL-1 saturates, the response to LMB is approximately linear with respect to the EGFP·RELA expression level. The maximum absolute translocation rate in response to LMB is higher than that in IL-1-stimulated cells, indicating that the limiting factor in the latter is not the import apparatus. Furthermore, the effects of IL-1 plus LMB are clearly greater than additive, indicating increased nuclear to cytoplasmic transport of EGFP·RELA following IL-1 stimulation. However, blocking the nuclear export pathway does not significantly reduce the saturability of IL-1-induced nuclear translocation of EGFP·RELA at high expression levels (Fig. 1*D*), suggesting that the restriction is within the signal transduction pathway.

To further analyze the response to LMB, we have determined its effects on the inhibitory protein IκBα. Treatment of cells with LMB induces the nuclear translocation of IκBα·EGFP (Fig. 2*A*). This is in contrast to IL-1, which induces its degradation (data not shown). However, the time dependence of IκBα·EGFP translocation is distinct from that for EGFP·RELA (Fig. 2*B*); it is more rapid and distinctly nonlinear. The concentration dependence of translocation is also moderately nonlinear, being reduced in cells expressing the highest levels (Fig. 2, *C* and *D*). However, this nonlinearity is only evident in cells with translocation rates above 0.5, rates that are not attained in the EGFP·RELA-transfected cells; so it is possible that a similar nonlinearity may in principle apply for EGFP·RELA translocation. (We cannot analyze cells with higher levels of EGFP·RELA expression because these display constitutive nuclear localization.)

The nuclear translocation of NFκB is intimately linked with activation of responsive genes. However, in contrast to the effects of LMB, stimuli that activate NFκB generally do so as a consequence of degradation of IκBα. Therefore, we have investigated whether the nuclear translocation induced by LMB results in activation of NFκB, using production of the NFκB-responsive cytokine IL-6 as a reporter. We find that whereas treatment with IL-1 results in marked increase of IL-6 production, there is no change following treatment with LMB (Fig. 3). Although treatment with IL-1 and LMB together results in enhanced translocation of NFκB as compared with treatment with IL-1 alone, it yields reduced activation, presumably because nuclear NFκB·IκB complexes are less susceptible to degradation than those in the cytoplasm. Thus, although LMB induces the nuclear accumulation of NFκB, this is in an inactive form.

In considering the effects of LMB, we suggest that the data can be accounted for by three types of mechanism (Fig. 4). First, IκB and NFκB might enter the nucleus as a complex. Second, IκB and NFκB might dissociate within the cytoplasm, thereby exposing their nuclear import signals, be imported to the nucleus independently, and then reassociate. Finally, degradation of IκB may liberate free NFκB, which translocates

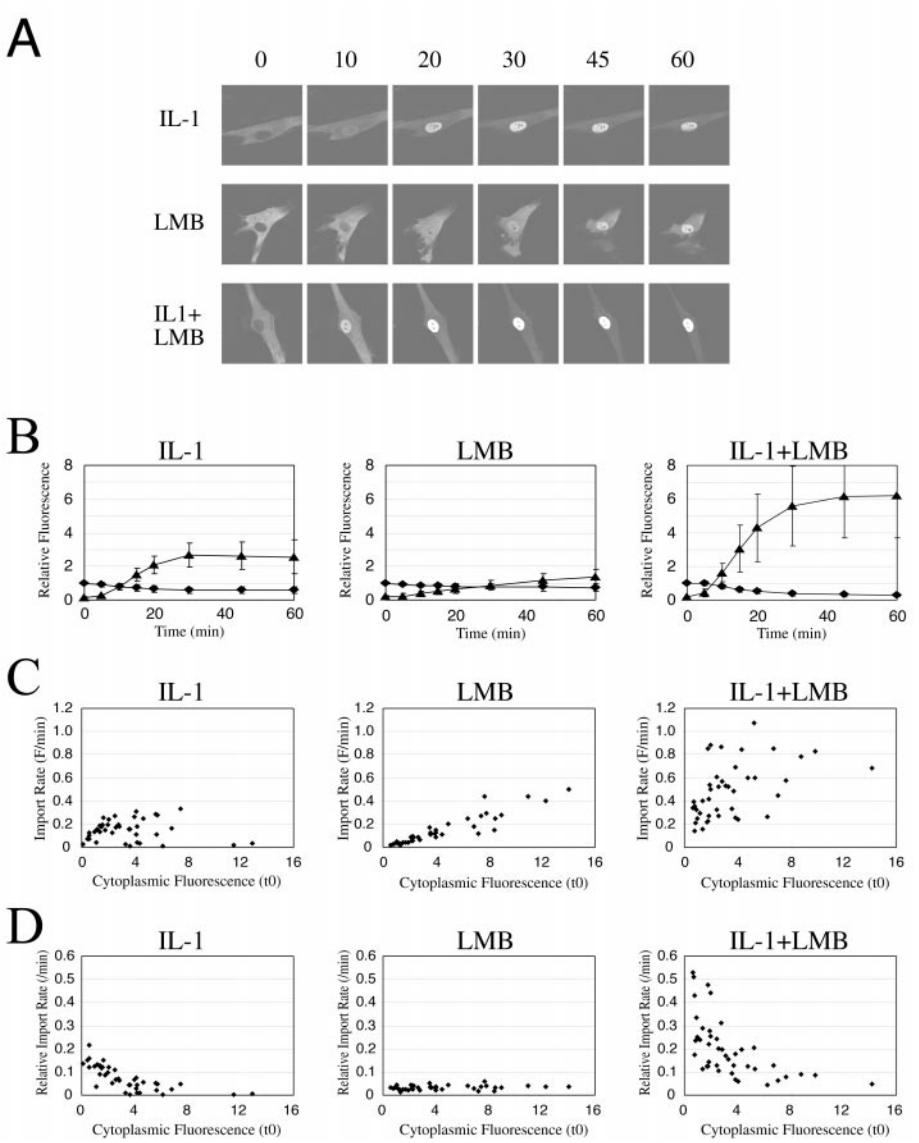

FIG. 1. **Analysis of EGFP·RELA redistribution.** *A*, translocation of EGFP·RELA from the cytoplasm to the nucleus occurs following treatment with IL-1 (1 nM) and/or LMB (10 ng/ml). Images show successive confocal sections of representative low level transfected cells taken 0, 10, 20, 30, 45, or 60 min after addition of IL-1 and/or LMB as indicated. *B*, quantitative determination of the mean time course of nuclear (▲) and cytoplasmic (♦) EGFP·RELA concentration following treatment with IL-1 and/or LMB for low level (relative fluorescence < 2) transfected cells. *Error bars* indicate 1 S.D. of the data. *C*, determination of the variation of the maximum rate of nuclear translocation in individual cells according to their initial cytoplasmic EGFP·RELA concentration, following treatment with IL-1 and/or LMB. *D*, determination of the relative import rates following treatment with IL-1 and/or LMB. *F*, flourescence units; *t0*, prestimulated levels.

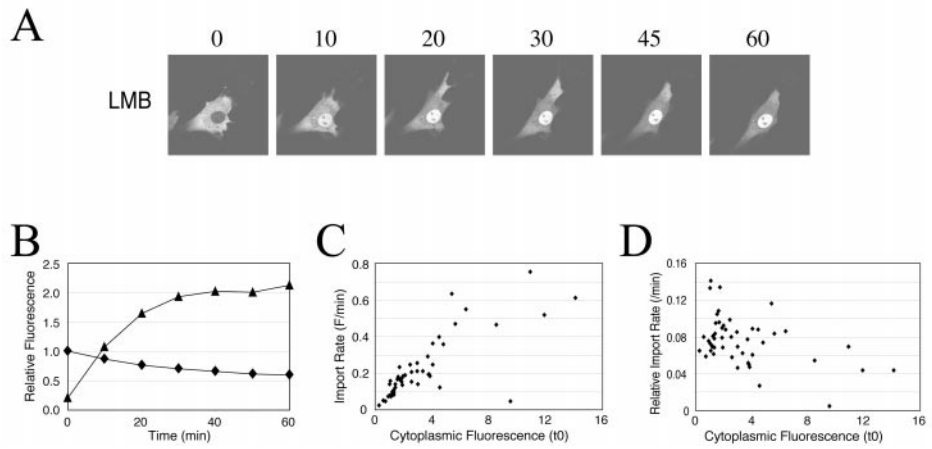

FIG. 2. **Analysis of IκBα·EGFP redistribution.** *A*, translocation of IκBα·EGFP from the cytoplasm to the nucleus following treatment with LMB (10 ng/ml). Images show successive confocal sections of a representative low level transfected cell taken 0, 10, 20, 30, 45, or 60 min after addition of LMB. *B*, quantitative determination of the mean time course of nuclear (▲) and cytoplasmic (♦) IκBα·EGFP concentration following treatment with LMB. *C*, determination of the variation of the maximum rate of nuclear translocation in individual cells according to their initial cytoplasmic IκBα·EGFP concentration. *D*, determination of the relative import rates following treatment with IL-1 and/or LMB. *F*, fluorescence units; *t0*, prestimulated levels.

into the nucleus, where it associates with newly synthesized IκB. We designed the following experiments to distinguish between these mechanisms.

Upon IL-1 stimulation, IκB is degraded by a proteasome-dependent pathway that is sensitive to the inhibitor MG132. To determine whether low intensity basal activation of this pathway is responsible for the shuttling of RELA and IκB, cells were treated with LMB and IL-1 in the presence of MG132 (Fig. 5, *A* and *B*). The degradation of IκBα and translocation of RELA in response to IL-1 are blocked by MG132, but their shuttling is not. Whereas this eliminates proteasome-dependent degradation of IκB, other pathways of protein degradation may be involved. Therefore, we determined whether new protein synthesis is required to sustain the cytoplasmic localization of RELA by treating cells with the protein synthesis inhibitor cycloheximide. There was no translocation of RELA to

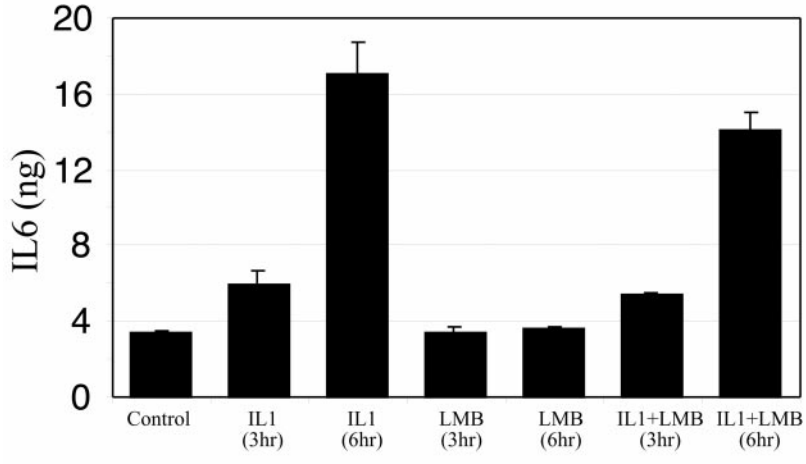

FIG. 3. **Modulation of IL-6 expression.** Cells were untreated or treated for the indicated times prior to assay with IL-1β (1 nM) or LMB (10 ng/ml); then production of I-6 was determined by enzyme-linked immunosorbent assay. The *error bars* indicate the standard deviation of the data.

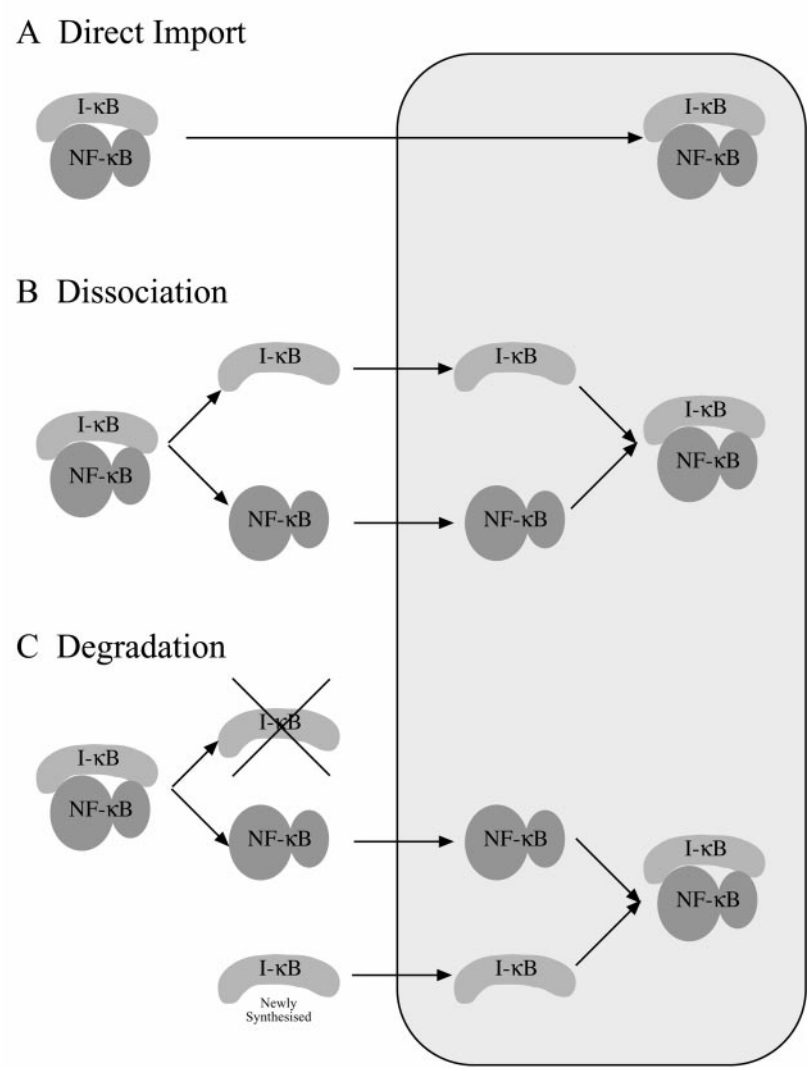

FIG. 4. **Proposed alternative models for the nuclear uptake of IκB and NFκB following treatment of cells with LMB.**

the nucleus within the time frame of our assays (data not shown), so the degradation-resynthesis mechanism of RELA/IκB cycling can be eliminated.

To distinguish between the remaining mechanisms, we examined the effect of free IκBα on the nuclear translocation of RELA in LMB-treated cells. If the basis of the translocation is dissociation, then increasing the concentration of free IκBα should reduce the rate of translocation because it will compete with the nuclear import machinery for free NFκB. It is not possible to obtain a direct measurement of free cytoplasmic IκBα, but it can be inferred from the nuclear IκBα concentration because NFκB-bound IκBα is predominantly cytoplasmic, whereas free IκBα distributes between the nucleus and cytoplasm in a 2:1 ratio.[2] Furthermore, by using ECFP·RELA plus IκBα·EYFP-transfected cells we can both measure the nuclear translocation rate of RELA and estimate the relative concentration of free cytoplasmic IκBα. Performing this experiment with cells expressing increasing amounts of IκBα·EYFP, we

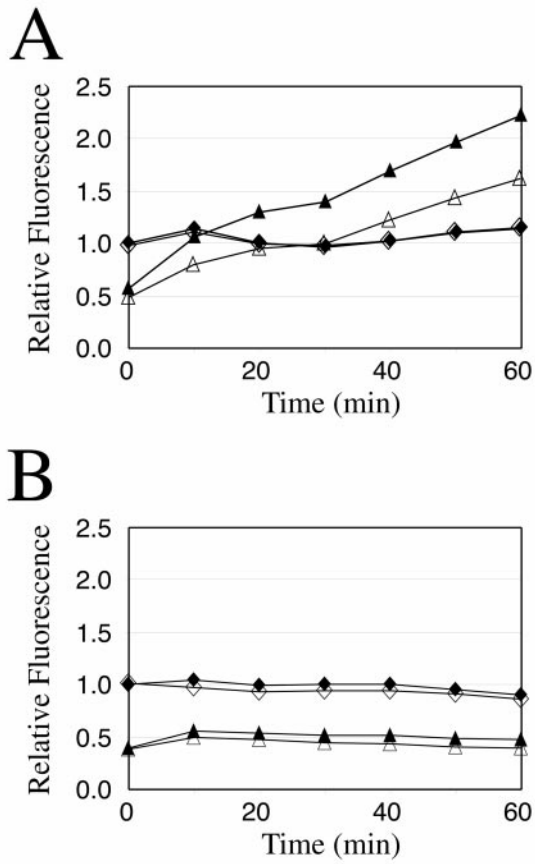

FIG. 5. **Simultaneous analysis of ECFP·RELA and IκBα·EYFP localization.** *A*, nuclear import following treatment with LMB (10 ng/ml) is not blocked in the presence of the proteasome inhibitor MG132 (50 μM). *B*, nuclear import of ECFP·RELA and degradation of IκBα·EYFP following treatment with IL-1β (1 nM) are blocked in the presence of MG132 (50 μg/ml). △, nuclear ECFP·RELA; ◇, cytoplasmic ECFP·RELA; ▲, nuclear IκBα·EYFP; ◆, cytoplasmic IκBα·EYFP.

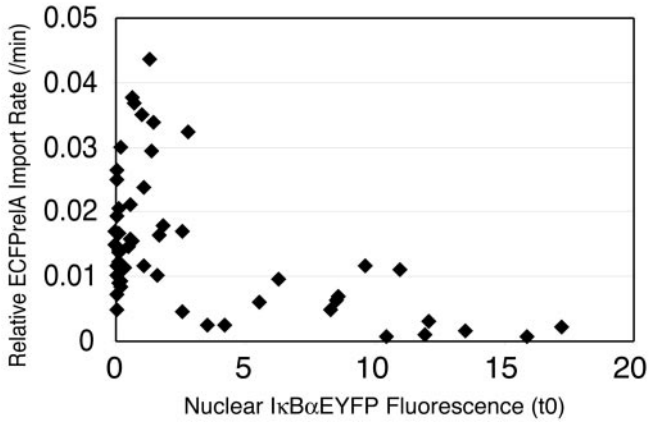

FIG. 6. **Variation in the relative rate of ECFP·RELA nuclear import following LMB (10 ng/ml) treatment according to initial nuclear IκBα·EYFP expression level.** Cells were transfected with *pECFP-RELA* plus *pIκBαEYFP*, and cells with increasing concentrations of nuclear (free) IκBα·EYFP were analyzed. The initial distribution of ECFP·RELA is predominantly cytoplasmic in all the cells analyzed, whereas that of IκBα·EYFP varies from predominantly cytoplasmic to predominantly nuclear as its expression level increases. *t0*, prestimulated levels.

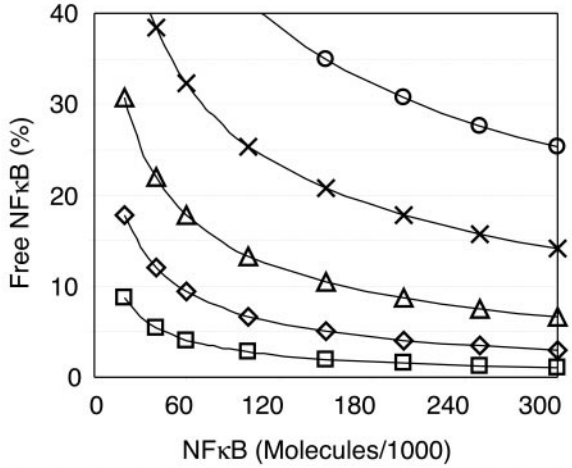

FIG. 7. **Free NFκB according to level of expression.** The expected percentage of free cytoplasmic NFκB, in the absence of nuclear-cytoplasmic shuttling, is shown at K_d values for the NFκB·IκB complex of 30(○), 10 (×), 3 (△), 1 (◇), and 0.3 nM (□).

found that those cells with the highest level of nuclear IκBα expression showed a reduced rate of ECFP·RELA import (Fig. 6). We do not believe this is due to competition between IκBα and NFκB at the nuclear pore, because the expression levels are within the linear range of LMB-induced nuclear accumulation (Figs. 1 and 2). Therefore we conclude that the basis for the nuclear-cytoplasmic shuttling is dissociation of the NFκB·IκB dimer within the cytoplasm and independent import of the subunits into the nucleus.

The theoretical validity of this dissociation/reassociation mechanism hinges on the dynamics of NFκB·IκB interactions within the cell. We have previously estimated the intracellular concentration of RELA to be 50 nM (60,000 molecules per cell; volume, 2,000 μm^3) (18). The dissociation constant of IκBα for various NFκB dimers has also been determined; the strongest interaction (3 nM) occurred with the RELA-p50 heterodimer (23). If we assume that NFκB is predominantly present as a RELA-p50 heterodimer and that IκBα is present in a small excess, then we predict that ~17% of cellular NFκB is free of IκB (by substitution into the equation $[NF\kappa B]\cdot[I\kappa B] = K_d\cdot[NF\kappa B\cdot I\kappa B]$). The presence of so much free NFκB was unexpected, so we examined how the predicted pool of free NFκB varies if the concentration and K_d estimates are modified (Fig. 7). We have previously estimated that the ratio of nuclear: cytoplasmic concentration is 1:10 and that the ratio of their volumes is also 1:10. Therefore, if the predominant function of IκBα is to retain NFκB in the cytoplasm by masking of its nuclear translocation signal, it would be necessary to have no more than 1% uncomplexed NFκB. To obtain a level of free NFκB this low, the estimated concentration/dissociation constant would have to be incorrect by at least 50-fold (Fig. 7).

We have considered a simple equilibrium process above, but the actual percentage of free NFκB will be determined by the dynamic equilibrium established between the association/dissociation of NFκB·IκB complexes, the import of free subunits into the nucleus, and the export of associated complexes to the cytoplasm. We propose that rapid export of NFκB·IκB complexes from the nucleus is necessary to maintain the low nuclear concentration of NFκB due to the non-saturated interaction between NFκB and IκB. To investigate the theoretical validity of this mechanism of NFκB/IκB function and better understand the proposed dynamic regulation of NFκB distribution, we developed a model based upon it. Essentially, our model considers two processes: association and dissociation of the NFκB·IκB complexes and import and export of the individual subunits and of the complex from the cytoplasm to the nucleus (Fig. 8). Firstly, we have investigated whether the model can account for the nuclear:cytoplasmic distribution of

NFκB using the reported concentration of RELA and affinity constant for interaction with IκBα. We found that two parameters are critical, namely the rate of import of IκB and export of the NFκB·IκB complex (Fig. 9*A*) and that, provided these are high enough, the model correctly simulates the distribution. Importantly, the underlying role of IκBα is in part to inhibit the nuclear translocation of NFκB and in part to facilitate its nuclear export; neither alone is sufficient. The predictions generated by the model correlate with our experimental results, with one exception; the relative translocation rate predicted at increasing NFκB expression levels is markedly more concentration-dependent than that of the experimental observations (Fig. 9*B*). This difference might be explained in two ways. First, it could also be a consequence of exhaustion of the endogenous p50 subunits, resulting in the formation of lower affinity complexes of IκBα with EGFP·RELA homodimers (K_d = 82 nM (23)). Alternatively, the off rate for the NFκB·IκB complex may be lower than the estimate we used, which would also be in accord with the ability to readily detect complexes by methods such as immunoprecipitation following cell lysis.

Whereas the dynamic model we are proposing is fundamentally very similar to the currently accepted static model, there are potentially important functional differences. First, the free nuclear NFκB concentration increases more gradually as IκB becomes sub-stoichiometric to NFκB, potentially facilitating graded, as opposed to on/off, activation of NFκB (Fig. 9*C*). This might have implications for the expression of certain genes at low levels of NFκB activation, in particular the regulation of basal IκBα expression. Second, alterations of the dynamics of the NFκB·IκB interaction can have a pronounced impact on free nuclear NFκB levels (Fig. 9*D*). This might be important in the differential regulation of NFκB by alternate members of the IκB gene family or by stimuli that modify IκBα without resulting in its degradation.

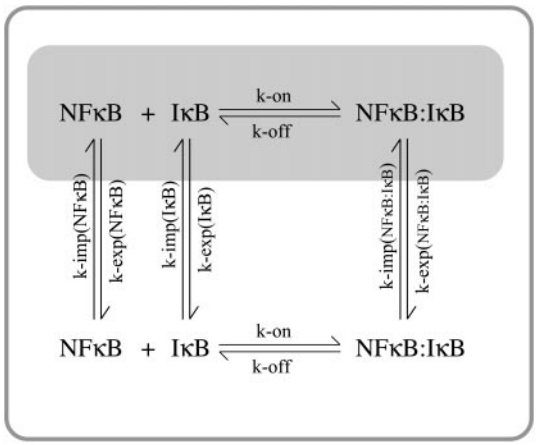

FIG. 8. **Model for NFκB and IκB nuclear-cytoplasmic distribution.** The programmed model consists of 6 variables (NFκB, IκB, and NFκB·IκB concentrations in the nucleus and cytoplasm) and 10 processes as illustrated. Each pair of processes was examined in turn, and their net alteration of the affected variables during the programmed time interval was determined. By performing sufficient iterations with a small enough time interval, dynamic equilibrium conditions can be established for a given set of parameters.

DISCUSSION

Much attention is currently being focused on understanding the process of signal transduction in mammalian cells. This work has resulted in the elucidation of a number of pathways, such as the IL-1/NFκB pathway studied in this report. To fully understand how these pathways function, we believe it is necessary to develop numerical models that accurately reflect their properties, and we have therefore used modelling to examine the consistency of our data with the suggested mechanism. Currently, our model is limited to the unstimulated partitioning of NFκB/IκB, but this core can be elaborated to model their redistribution following signal-induced modification/degradation of IκB. Whereas it is true that without exact knowledge of the parameter values the model is only a "guess," useful insights can still be gained, and the parameters needing to be measured can be better defined.

One aspect common to many characterized signal transduction pathways is the involvement of sequentially acting kinases. These steps each have the potential for significant amplification, suggesting that the complete pathway may be subject to a large degree of amplification. However, our previous work has identified a modest limiting rate for nuclear translocation of EGFP·RELA that we suggested may either be

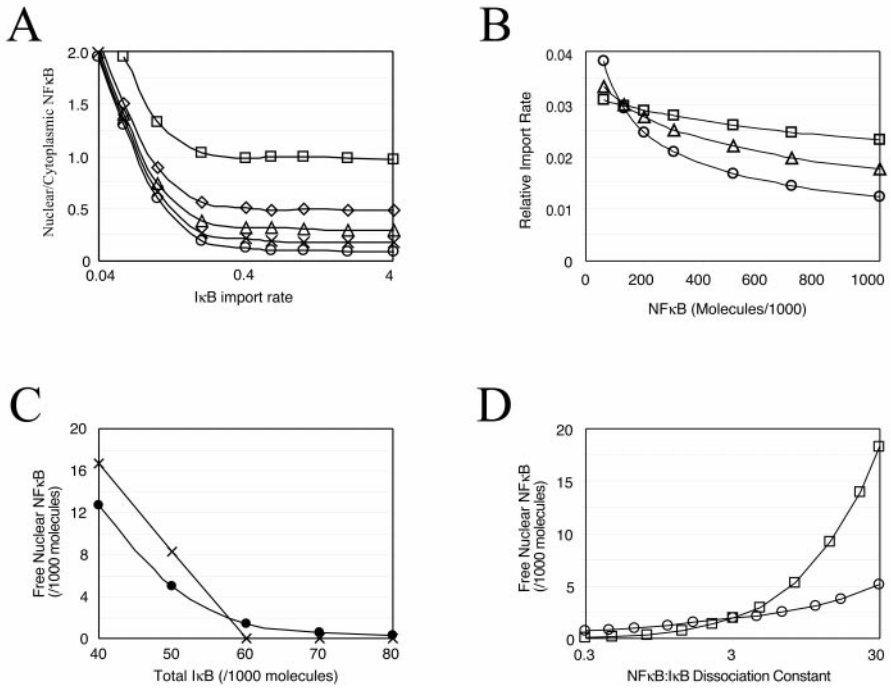

FIG. 9. **Modelling of parameter values.** *A*, predicted nuclear/cytoplasmic NFκB ratio under conditions of dynamic equilibrium. The effect of the IκB import rate is shown for NFκB·IκB export rates of 0.045 M^{-1} s^{-1} (□), 0.1 M^{-1} s^{-1} (◇), 0.2 M^{-1} s^{-1} (△), 0.45 M^{-1} s^{-1} (×), and 4.5 M^{-1} s^{-1} (○). *B*, variation of the predicted nuclear import rate of NFκB in LMB-treated cells *versus* NFκB expression level at k_{off} values of 0.055 (○), 0.0055 (△), and 0.0035 s^{-1} (□). *C*, variation of free nuclear NFκB *versus* IκB expression assuming equilibrium (●) or saturation (×) models. *D*, variation of free nuclear NFκB *versus* dissociation constant as a result of varying k_{off} (○) or k_{on} (□).

due to limitations in the signal transduction pathway or the NFκB nuclear import process. The present data substantiate the conclusion that the limitation is at or upstream of IκBα degradation and not a consequence of limitations on the rate of nuclear import of free NFκB.

Our experiments, in accord with other recent reports (24, 25), demonstrate that the cytoplasmic localization of NFκB in resting cells is not static but instead the result of balancing fluxes into and out of the nucleus. We demonstrate that the underlying cause for basal RELA and IκBα nuclear-cytoplasmic shuttling is the dissociation of IκB·NFκB complexes as opposed to their direct nuclear import or degradation and resynthesis of IκBα. This mechanism is consistent with the previously determined affinity of the IκB-NFκB interaction, which predicts sequestration of ~83% of NFκB dimers into inactive complexes. Without the nuclear export function of IκBα, the potential activation of NFκB following IκBα degradation is approximately 6-fold. However, the combined action of IκB-dependent nuclear export and formation of inactive complexes gives much lower residual nuclear activity and hence much more stringent regulation.

Because nuclear import and export are energy-dependent processes, the futile cycle of NFκB import to and export from the nucleus would appear to be energetically inefficient. Why should the system be designed in this manner when, with a higher affinity of interaction between IκB and NFκB, nuclear-cytoplasmic shuttling would be unnecessary? With two inhibitory steps (export and anchoring), the activity is more sensitive to small changes in the extent of interaction because the inhibition is proportional to the square of IκB-bound NFκB. If the binding between two molecules is near saturation, a small change in the affinity constant would have negligible effects on their free concentrations; however, under conditions of lower saturation, the same change can have a greater influence on the degree of interaction. This might be important in the differential interaction of the various NFκB dimers with specific IκBs. By keeping the dissociation constant high, specificity of inhibition can be better achieved.

Association/dissociation of the inhibitor may also allow for alteration in the nature of the complexes under different growth conditions or following transient activation of the inflammatory response. For example, following activation of NFκB, the synthesis of IκBα is induced. Hence, shortly after inactivation there may be a predominance of inhibitory complexes containing IκBα that are subsequently displaced by other inhibitors. This change may coincide with either greater or lesser sensitivity to specific inducing agents. In addition, it has been reported that IκBα is controlled under some circumstances by tyrosine phosphorylation, which results in dissociation but not degradation (13, 26). As discussed above, this mechanism is more tenable if the affinity of the complex is relatively low. Similar to the results reported here, recent analysis of the interaction of the glucocorticoid receptor with DNA has demonstrated rapid exchange between bound and free pools within living cells (27). Therefore, dynamic interactions involving transcription factors are probably common within living cells.

In conclusion, we propose that the regulation of NFκB is dependent on dynamic shuttling between the nucleus and cytoplasm and that underlying this shuttling is dissociation of the transcription factor and inhibitor within the cytoplasm. The numerical model we have developed accurately simulates many aspects of the nuclear-cytoplasmic distribution of NFκB but identifies areas of inconsistency for future research. Whereas it is well established that IκBα expression is induced by RELA overexpression, determination of precisely how the expression level of IκBα relates to the level of RELA is important to refine our model. Elaboration of the model to consider different NFκB dimers and other IκBs is also necessary but can only be achieved following characterization of their kinetics of interaction. Finally, direct measurement of the rate of nuclear import and export of specific complexes will also be required.

Acknowledgments—We thank the Immunex Corporation (Seattle, Washington) for the gift of IL-1β and Minoru Yoshida (Department of Biotechnology, University of Tokyo) for the gift of LMB.

REFERENCES

1. Verma, I. M., Stevenson, J. K., Schwarz, E. M., Vanantwerp, D., and Miyamoto, S. (1995) *Genes Dev.* **9**, 2723–2735
2. Ghosh, S., May, M. J., and Kopp, E. B. (1998) *Annu. Rev. Immunol.* **16,** 225–260
3. Bours, V., Franzoso, G., Azarenko, V., Park, S., Kanno, T., Brown, K., and Siebenlist, U. (1993) *Cell* **72,** 729–739
4. Fujita, T., Nolan, G. P., Liou, H. C., Scott, M. L., and Baltimore, D. (1993) *Genes Dev.* **7,** 1354–1363
5. Beg, A., and Baldwin, A. S. (1993) *Genes Dev.* **7**, 2064–2070
6. Baeuerle, P. A., and Baltimore, D. (1988) *Science* **242**, 540–546
7. Jacobs, M. D., and Harrison, S. C. (1998) *Cell* **95,** 749–758
8. Sen, R., and Baltimore, D. (1987) *Cell* **47,** 921–928
9. Osborn, L., Kunkel, S., and Nabel, G. J. (1989) *Proc. Natl. Acad. Sci. U. S. A.* **86**, 2336–2340
10. Beg, A. A., Finco, T. S., Nantermet, P. V., and Baldwin, A. S. (1993) *Mol. Cell. Biol.* **13**, 3301–3310
11. Traenckner, E., Pahl, H., Henkel, T., Schmidt, K., Wilk, S., and Baeuerle, P. (1995) *EMBO J.* **14**, 2876–2883
12. Henkel, T., Machleidt, T., Alkalay, I., Kronke, M., Ben-Neriah, Y., and Baeuerle, P. (1993) *Nature* **365**, 182–185
13. Imbert, V., Rupec, R. A., Livolsi, A., Pahl, H. L., Traenckner, E. B. M., Mueller-Dieckmann, C., Farahifar, D., Rossi, B., Auberger, P., Baeuerle, P. A., and Peyron, J. F. (1996) *Cell* **86,** 787–798
14. Wang, D., and Baldwin, A. S. (1998) *J. Biol. Chem.* **273,** 29411–29416
15. Zhong, H., SuYang, H., Erdjument-Bromage, H., Tempst, P., and Ghosh, S. (1997) *Cell* **89,** 413–424
16. Bergmann, M., Hart, L., Lindsay, M., Barnes, P., and Newton, R. (1998) *J. Biol. Chem.* **273**, 6607–6610
17. Bird, T. A., Schooley, K., Dower, S. K., Hagen, H., and Virca, G. D. (1997) *J. Biol. Chem.* **272,** 32606–32612
18. Carlotti, F., Chapman, R., Dower, S. K., and Qwarnstrom, E. E. (1999) *J. Biol. Chem.* **274,** 37941–37949
19. Kudo, N., Khochbin, S., Nishi, K., Kitano, K., Yanagida, M., Yoshida, M., and Horinouchi, S. (1997) *J. Biol. Chem.* **272,** 29742–29751
20. Rodriguez, M. S., Thompson, J., Hay, R. T., and Dargemont, C. (1999) *J. Biol. Chem.* **274,** 9108–9115
21. Chiao, P. J., Miyamoto, S., and Verma, I. M. (1994) *Proc. Natl. Acad. Sci. U. S. A.* **91**, 28–32
22. Sun, S. C., Ganchi, P. A., Ballard, D. W., and Greene, W. C. (1993) *Science* **259**, 1912–1915
23. Malek, S., Huxford, T., and Ghosh, G. (1998) *J. Biol. Chem.* **273,** 25427–25435
24. Huang, T. T., Kudo, N., Yoshida, M., and Miyamoto, S. (2000) *Proc. Natl. Acad. Sci. U. S. A.* **97,** 1014–1019
25. Johnson, C., Van Antwerp, D., and Hope, T. J. (1999) *EMBO J.* **18,** 6682–6693
26. Chu, Z.-L., McKinsey, T. A., Liu, L., Qi, X., and Ballard, D. W. (1996) *Mol. Cell. Biol.* **16,** 5974–5984
27. McNally, J. G., Muller, W. G., Walker, D., Wolford, R., and Hager, G. L. (2000) *Science* **287,** 1262–1265